RSC Advances

ROYAL SOCIETY OF CHEMISTRY

www.rsc.org/advances

Journal Name

RSCPublishing

ARTICLE

Combination of Hematin and PEDOT via 1-Pyrenebutanoic acid: A new platform for direct electrochemistry of hematin and biosensing applications

Cite this: DOI: 10.1039/x0xx00000x

Received 00th January 2014,
Accepted 00th January 2014

DOI: 10.1039/x0xx00000x

www.rsc.org/

X.H. Yu[1], J.M. Kong[1*], X.J. Han[2] and X.J. Zhang[1,3*]

Abstract: In this work, we prepare a novel platform based on Poly(3,4-ethylenedioxythiophene)(PEDOT) and 1-Pyrenebutanoic acid (PBA). PEDOT is a conductive material of heteroatom doping, which can connect with PBA through π–π stacking. Feasibility of the film is testified via fabricating it on glassy carbon electrode (GCE), then linked hematin with PBA via carboxylate-zirconium-carboxylate coordination bond to prepare GCE/PEDOT/PBA/Hematin biosensor. The electrochemical performance of the biosensor has been tested by Electrochemical Impedance Spectroscopy (EIS), Cyclic voltammetry (CV) and Current-Time curve method (I-T). From CV, a pair of well-defined and quasi-reversible redox peaks, corresponding to the hematin Fe(III)/Fe(II) redox couple is observed, and the surface coverage (Γ*) of hematin on GCE has been calculated to be 1.2×10^{-9} mol·cm^{-2}, which is almost 20 times larger than the monolayer coverage of hemin. This value shows that the PEDOT and PBA composite lead to a better loading of the hematin on the surface of GCE. In addition, GCE/PEDOT-PBA-Hematin biosensor exhibits strong electro-catalysis activity for H_2O_2 and displays a linear response for the reduction of H_2O_2 in the range of 0.005 to 1.322 mmol·L^{-1}, with a detection limit of 0.03 μmol·L^{-1},high sensitivity of 2.83 μA·mM^{-1}·cm^{-2}.In addition, the sensor has also been applied to the determination of H_2O_2 in real samples, and the response is in the ideal range, which means that the GCE/PEDOT-PBA-Hematin biosensor is very useful in the future application.

1 Introduction

Porphyrins have been found wide applications as redox catalysts in numerous chemical processes. Hemin is one of porphyrins, which is the active center of hemoglobin and several other enzymes, contained in proteins in a blood corpuscle.[1]Hematin is the hydroxylated hemin, which exhibits strong electrocatalysis to oxygen, peroxide, nitric oxide, carbon dioxide, and hydrogen peroxide.[2-6]The catalytic activities come from the redox reaction of the ferric/ferrous ion in the center of hematin. However, as a biomimetic catalyst, the catalytic activity and stability of hematin is inferior to natural enzymes.[7] In recent years, large numbers of reports have been dedicated to improve the catalytic performance of hematin;[8-11] generally carbon nanotubes or graphenes have been used to immobilize hematin. Experiments indicated that carbon materials can greatly promote the catalytic activities of hematin.[9-11]However, these materials suffer from drawbacks such as cumbersome preparation methods, indirect detection procedure and so on.

In 2001, Chen proposed the method for immobilizing proteins and small biomolecules on carbon nanotubes by 1-Pyrenebutanoic acid (PBA). PBA contains four benzene rings, it is known that PBA can interact strongly with carbon nanotubes and graphene via π–π stacking.[12,13]Many studies focused on the way of immobilizing various enzymes and proteins on carbon materials via PBA.[14-17]However, carbon nanotubes and graphenes are expensive and the procedures for preparation is also troublesome. Aiming at a simple and stable basement to immobilize hematin, we take efforts to find a material, which can connect with PBA via π–π stacking. PEDOT is one of the most studied conducting polymers,[18,19] its good stability, high-speed electron transfer, and easy formation of tenacious film make it a good material for sensor. First of all, PEDOT is a conductive material of heteroatom doping, it can serve as a versatile building block for advanced functional π-conjugated systems due to the amounts and geometry of benzene ring contained in PEDOT.[20]Based on above considerations, for the first time we use PEDOT together with

PBA fabricating a new type of hematin electrochemical biosensor. In this approach, PBA is irreversibly adsorbed on the hydrophobic surfaces of PEDOT film via π–π stacking, and carboxyl groups in PBA are introduced on glassy carbon electrode (GCE) surface, which is easy to connect hematin via coordinate bond of carboxylate-zirconium-carboxylate.[21-24]The association of hematin to PBA is illustrated in **Scheme 1**.

In general, H_2O_2 involves in many biological processes. H_2O_2 participates in a wide range of enzymatic reactions particularly, plays an important role in biological processes such as the metabolism of proteins and carbohydrates or in immune responses;[25] meanwhile it is associated with the diagnostic response in several biochemical methods for monitoring blood glucose.[26] H_2O_2 is also utilized in many industrial processes such as the manufacture of pharmaceuticals, treatment of paper, textiles and food.[27,28] Therefore, analysis of H_2O_2 is essential in clinical and industrial samples. Here we report a new sensitive biomimetic sensor based on PEDOT, PBA and hematin for H_2O_2 detection.

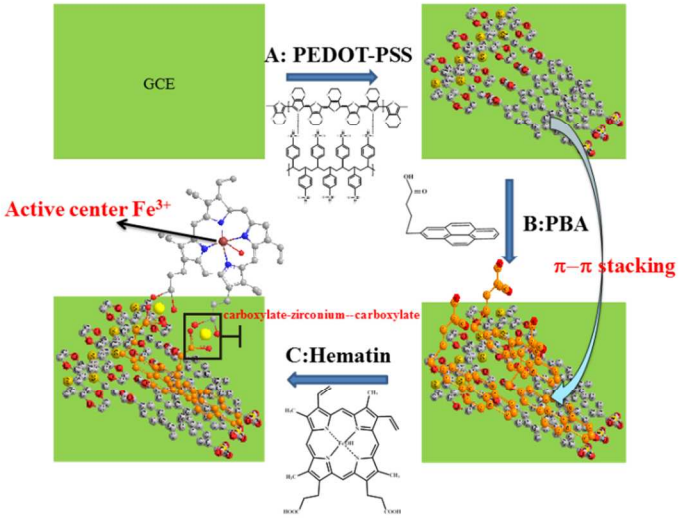

Scheme 1 Mimetic diagram of the electrochemical sensor preparation. (A) Polymerize EDOT to the surface of GCE; (B) The PBA connect with PEDOT via π–π interaction; (C) Hematin to the functionalized film through Carboxylic-Zirconium-Carboxylic.(red:O; dark yellow:S; gray: C; yellow: Zr; blue: N; brown: Fe; orange ring:PBA)

2 Results and discussion

2.1 Characterization of GCEs with different modification by XPS and SEM

Characterization of GCE/bare, GCE/PEDOT, GCE/PEDOT-PBA and GCE/PEDOT-PBA-Hematin was implemented by XPS and SEM. All XPS spectra were taken after Ar ion gas etching for 50 s and corrected using a C1s peak at 284.6 eV as an internal standard. **Fig. 1** shows XPS and SEM images of these electrodes: (a) GCE/bare; (b)GCE/PEDOT; (c) GCE/PEDOT-PBA; (d) GCE/PEDOT-PBA-Hematin. Compared to Fig. 1(2) a, Fig. 1(2) b displays a surface topography with high roughness and loose structure; then from the results of XPS (Fig. 1(1) (A) and Fig. 1(1) (A1)), S peak and increased O peak were observed obviously; therefore, SEM and XPS together demonstrates that the PEDOT has been deposited onto the surface of GCE successfully. As shown in Fig. 1(1) (A) c, the same elements (C, O, S)was detected as Fig. 1(1) (A) b, because PBA is composed of C, H and O. We can deduce that PBA was connected with PEDOT through π-π stacking from SEM image (Fig. 1(2) c), its surface density was denser than GCE/PEDOT. As shown in Fig. 1(2) d, the GCE/PEDOT-PBA-Hematin film renders rough and dense with numerous protrusions that could be assigned to the deposition of hematin molecules with large aggregations. In addition, Zr, N and Fe were observed from XPS of GCE/PEDOT-PBA-Hematin, hence, it proved that hematin was linked with PBA. Integrating the results of SEM and XPS, we can find that a new GCE/PEDOT-PBA-Hematin sensor is formed as expected.

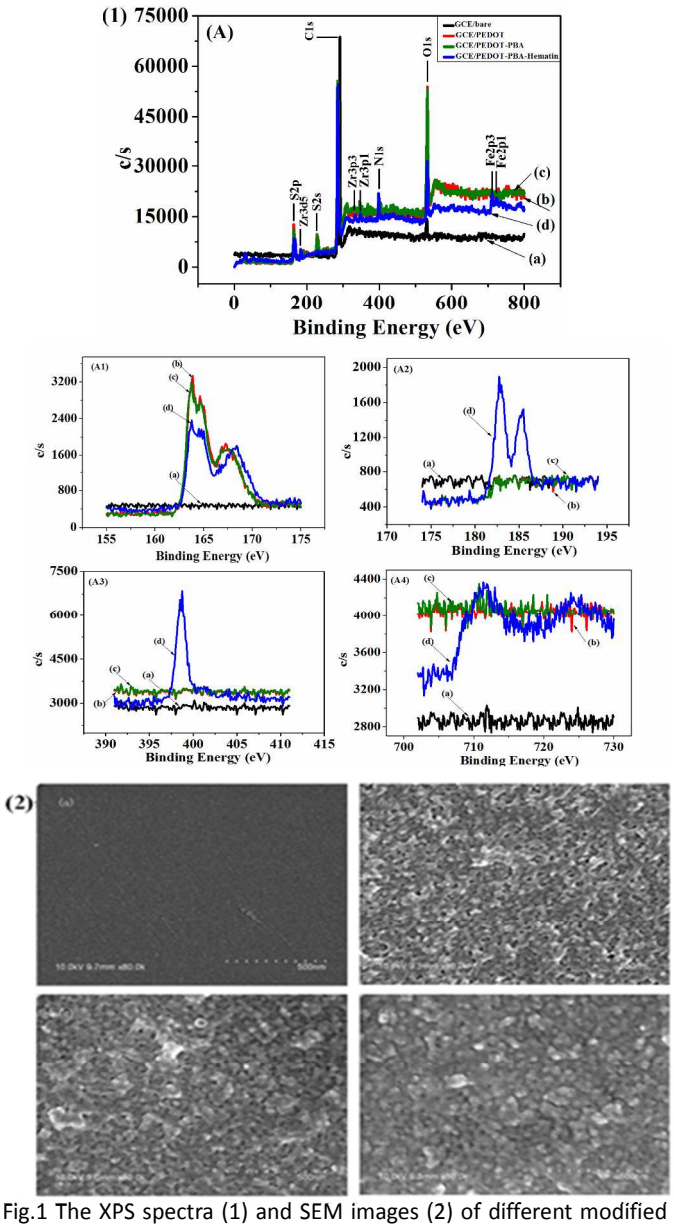

Fig.1 The XPS spectra (1) and SEM images (2) of different modified

GCEs: (a) GCE/bare; (b) GCE/PEDOT; (c) GCE/PEDOT-PBA; (d) GCE/PEDOT-PBA-Hematin, (A1) S peak; (A2) Zr peak; (A3) N peak; (A4) Fe peak.

2.2 EIS and CVs of different modified GCEs

Electrochemical impedance spectroscopy (**Fig. 2A**) and cyclic voltammograms (**Fig. 2B**) were carried out in 50 mmol·L^{-1} $Fe(CN)_6^{3-/4-}$ aqueous solution as the electro-active probe with 0.1 mol·L^{-1} KNO_3 supporting electrolyte and the reference electrode is saturated calomel electrode (the same below). The impedance technique can provide more detailed information about the interfacial properties of surface-modified electrode. **Fig. 2 A** shows the impedance responses of GCE modified with different layers, the open circuit potential was selected at 0.19 V with the frequency range from 10^{-2} Hz to 10^5 Hz for EIS experiments. Generally, there are two parts of result observed on an EIS plot: the first is a semicircular graph found at higher frequencies, which is related to the electron transfer-limited processes in a film; the second is a linear graph found at lower frequencies, resulting from the diffusion-limited processes in a film.[30] The diameter of the semicircle exhibited the electron transfer resistance of the layer, showing its blocking behavior for the interface properties of the electrode.

The impedance data were fitted with commercial software Autolab data analysis (Metrohm, Switzerland). A modified Randle's equivalent circuit,[31,32]as shown in Fig. 2C, was found to fit the data adequately over the entire measurement frequency range. The circuit includes following four elements: (i) the ohmic resistance of the electrolyte solution, R_S; (ii) CPE, associated with the double layer reflecting the interface between the assembled film and the electrolyte solution; (iii) R_P the electron transfer resistance.[33] Ideally R_S represent the properties of the electrolyte solution and diffusion of the redox probe, thus, it is not affected by modifications occurring on the electrode surface.[34] A negligible change in R_S was observed during either the deposition of PEDOT, the immobilization of PBA, or the coupling of hematin in the last procedure. At the same time, as can be seen in Fig. 2A, the changes in R_P were more significant than those in other impedance components. Thus, R_P was a suitable signal for sensing the interfacial properties of the GCE during all of those assembly procedures. The fitting values for the stepwise assembled layers on the electrode are presented in Fig.2C. For the bare GCE, the value for R_P is 134Ω, with a short diameter of the semicircular plot (Fig. 2A,a), a typical characteristic of a diffusion limited electron transfer process.[35]When EDOT was polymerized on GCE, the plot changed to effective linear relationship because of the fast electron transfer rate of PEDOT (Fig. 2A, b), with a decrease in the R_P value to 19.7Ω. A slight increase in the R_P value (to 36.5Ω) was observed after deposition of PBA to the PEDOT layer, and the R_P value was increased to 70.4Ω in the successive step of immobilization of hematin, which may results from the thickness increase of modification on GCE. When compared with GCE/Hematin (Fig. 2A, e), the R_P of GCE/PEDOT/PBA/Hematin decreased nearly 10 times compared to that of GCE/Hematin, which was owing to PEDOT playing a promoting role in electron transfer. Here PEDOT immobilized on the electrode played an important role similar to an electron-conducting tunnel, making electron transfer to the electrode surface easier. These results were consistent with those obtained by CV measurements.

CV is another essential method for studying interface properties of modified electrodes. The $[Fe(CN)_6]^{3-/4-}$ complex ions are electrochemical probes commonly utilized for the investigation of the construction of complex biosensors.[36] Well-defined oxidation and reduction peaks of $[Fe(CN)_6]^{3-/4-}$(Fig. 2B, a) were observed at the bare GCE. After the EDOT polymerized on the electrode, the peak current at the modified electrode increased (Fig. 2B, b); this was attributed to the good conductivity of the PEDOT, which could facilitate electron transfer between the conductive polymer and the electrode surface. When the GCE/PEDOT-PBA (Fig. 2B, c) and GCE/PEDOT-PBA-Hematin (Fig. 2B, d) were tested, it was found that the catalytic rate of the latter GCEs is higher. In contrast, when the GCE was treated merely with the hematin, the reversibility decreased compared to the bare GCE (Fig. 2B,e).This demonstrated that the hematin could impede the electron transfer between the bio-molecules and the electrode surface in some extent. However, when both the hematin and PEDOT were deposited on the GCE, the cathodic and anodic peak currents clearly increased (Fig. 2B, d),which is attributed to the good electrical conductivity of PEDOT.

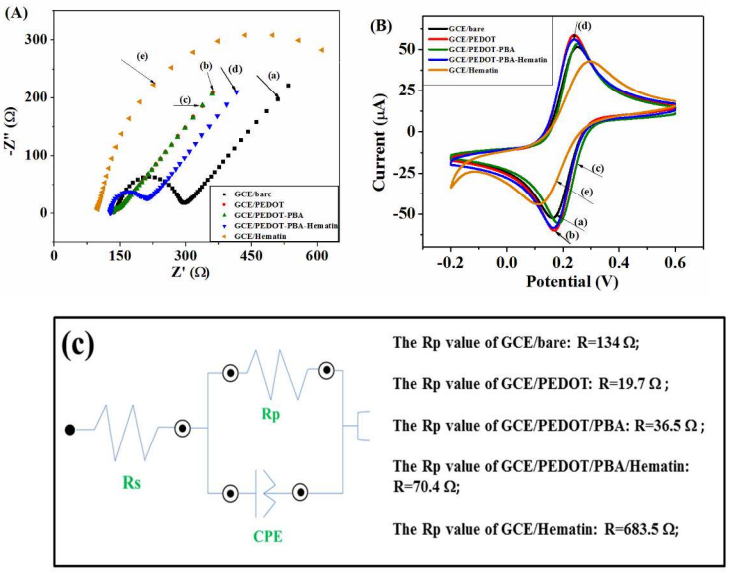

Fig. 2 (A) Electrochemical impedance spectroscopy and (B) cyclic voltammograms of CGE/bare (a); GCE/PEDOT (b); GCE/PEDOT-PBA (c); GCE/PEDOT-PBA-Hematin (d); GCE/Hematin (e) in 50 mmol·L^{-1} $Fe(CN)_6^{3-/4-}$ aqueous solution as the electro-active probe with 0.1 mol·L^{-1} KNO_3 as the supporting electrolyte. (C) A modified Randle's equivalent circuit of EIS. Potentials vs. to Hg/HgCl/Saturated KCl reference electrode.

(For interpretation of the references to color in this figure legend, the reader is referred to the web version of this article)

2.3 The catalytic effect to H_2O_2 at different modified electrodes

To investigate the performance of the five different types of electrode, cyclic voltammetry experiments were conducted at each

electrode immersed in 0.08 mmol·L^{-1} H_2O_2 in 0.1 mol·L^{-1} PBS buffer (pH 7.0), which was stirred and saturated by the bubbling N_2 gas. **Fig. 3** shows the typical CVs of different modified electrodes. There are no redox peaks appearing for the GCE/bare (Fig.3, a); GCE/PEDOT (Fig. 3, b) and GCE/PEDOT-PBA (Fig. 3, c). When the GCE was modified with hematin, an obvious cathodic peak was observed (Fig. 3, d and e), indicating that the redox response observed is due to the presence of hematin. As Fig. 3 shows, GCE/Hematin only yielded a negligible current response to the addition of 0.08 mmol·L^{-1} H_2O_2, indicating that the direct electron transfer between the hematin and the electrode is difficult. An obvious increase of current is observed in GCE/PEDOT/PBA/Hematin compared to GCE/Hematin, which was 3 times larger than that of GCE/Hematin. Different performance of electrodes are mainly attributed to the excellent properties of PEDOT. These conductive material of heteroatom doping individual sheets have good electrocatalytic activity towards H_2O_2, and the high surface area-to-volume ratio is favorable for hematin immobilization.

Earlier work suggests that the catalysis involves a ferric/ferryl redox cycle (Scheme 2). These circular reaction systems produce both alkoxyl (LO•) and peroxyl (LOO•) radical species.[37]Step 1: hematin reacts with (H_2O_2) to form ferryl hematin along with various radical species capable of oxidizing substrates such as the heme moiety, or the protein. Step 2: Protonation of the oxyferryl species to form [Fe^{4+}-OH^-]$^{3+}$ destabilizes the complex, giving it a radical-like nature. The box defined by the broken line depicts the protonated ferryl species and radical species electronically equivalent. Step 3: Auto-reduction of the protonated species occurs by abstraction of an electron, probably from the porphyrin ring.[38]

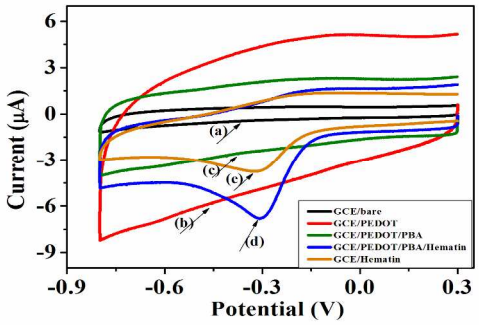

Fig. 3 The typical Cyclic voltammograms to H_2O_2 on different modified GCEs in 0.1 mol·L^{-1} PBS (pH7.0) which contains 0.08 mmol·L^{-1} H_2O_2: (a) GCE/bare; (b) GCE/PEDOT; (c) GCE/PEDOT-PBA; (d) GCE/PEDOT-PBA-Hematin; (e) GCE/Hematin. Potentials vs. to Hg/HgCl/Saturated KCl reference electrode.

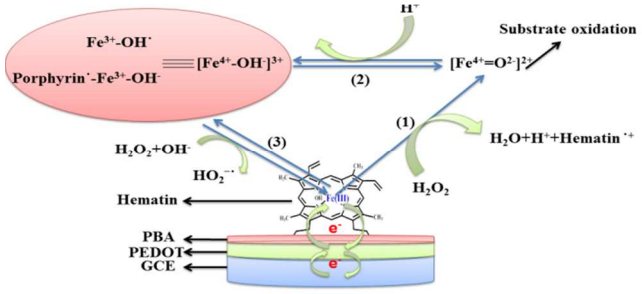

Scheme 2 Mechanism of peroxide-induced ferryl formation and subsequent auto-reduction.

2.4 The effect of scan rate on the direct electrochemistry of hematin on GCE/PEDOT-PBA-Hematin

The CVs of the modified electrodes at different scan rates are shown in **Fig. 4**. The redox peak current and the peak potential increased as a function of scan rate. The cathodic and anodic peak currents increased linearly with the scan rate from 20 to 300 mV·s^{-1}.For anodic peak current: I=3.823C-0.035, R=0.998; for cathodic peak current: I=-3.802C+0.034,R=0.999. It is clear that hematin was adsorbed on the surface and underwent a surface confined electron transfer;[39]its surface coverage (Γ^*) can be calculated according to the Laviron equation:[40]

$$I_p = \frac{N^2F^2\nu\Gamma^*A}{4RT} = \frac{NFQ\ \nu}{4RT}$$

Where I_p is the peak current, N is the number of electrons transferred (N=1),F is the Faraday constant, ν is the scan rate, A is the effective surface area (0.07 cm^2),Q is the quantity of charge(8.19×10^{-6}C), R is the gas constant and T is the temperature(298.15 K). From this equation, the surface coverage (Γ^*) was calculated to be 1.2×10^{-9} mol·cm^{-2}, which is larger than the theoretical monolayer coverage of Hb (6.98×10^{-11}mol·cm^{-2}) and is almost 20 times larger than the monolayer coverage of hemin.[41,42]This value shows that the PEDOT film and PBA lead to a better loading of the hematin on the surface of GCE, which enhances the electron transfer rate and catalytic ability of hematin.

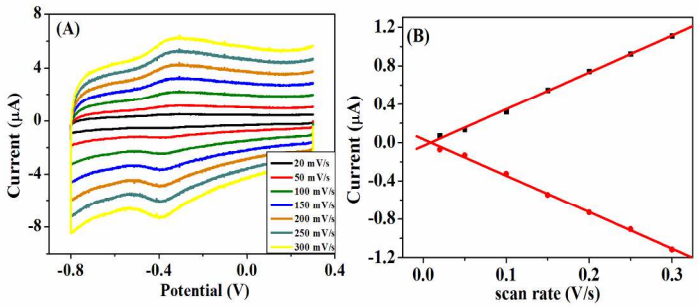

Fig. 4 (A) Cyclic voltammograms of GCE/PEDOT-PBA-Hematin in 0.1 mol·L^{-1} PBS (pH 7.0) with scan rates of 20–300 mV·s^{-1}. (B) Plots of cathodic and anodic peak currents versus scan rate. Potentials vs. to Hg/HgCl/Saturated KCl reference electrode.

2.5 The effect of pH on the catalysis of GCE/PEDOT-PBA-Hematin to H_2O_2

The pH value of the electrolyte is important for the performance of the biosensor. **Fig.5** shows the amperometric response of GCE/PEDOT-PBA-Hematin at different pH values (pH 5.0 to pH 9.0) in the presence of the 0.08 mmol·L^{-1} of H_2O_2. As can be seen from Fig. 5B, the response current decreased from pH5.0 and reached the minimum at pH 6.0, then increased with pH value from 6.0 to 7.0, then decreased quickly from pH7.4 to pH9.0.The maximal catalysis is at pH5.0. It may be attributed to the proton involving in the electrochemical reaction. In alkaline environment, the

electrochemical reaction becomes more difficult due to the lack of protons. However, in acidic media, hematin on GCE is not very stable, so we choose pH 7.0 as the optimal condition.[39,43]As shown in Fig. 5C, cathodic peak potentials (Epc) shifted negatively with pH increasing from 5.0 to 9.0. The Epc showed a linear response to pH from 5.0 to 9.0. The slope was about 40 (±2.6) mV per unit pH, which was smaller than the theoretical value of 57.6 mV per unit pH at 18℃ for a single-proton coupled and reversible one-electron transfer.[44] The potential at pH7.0 was -0.3V, which suggested that the groups near the heme iron made an impact on the redox potential.

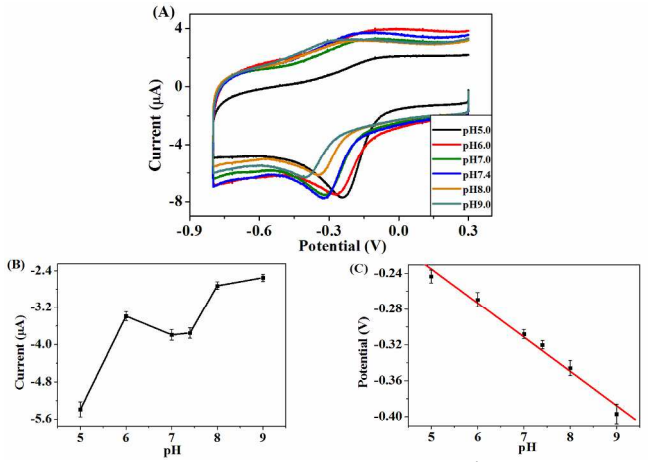

Fig. 5 (A) Cyclic voltammograms of GCE/PEDOT-PBA-Hematin measured in different pH values at 100 mV/s, with the present of 0.08 mmol·L^{-1} H_2O_2; (B) The change of current with different pH values; (C) The liner variation of potential with pH values. Potentials vs. to Hg/HgCl/Saturated KCl reference electrode.

2.6 Electrocatalytic activities to H_2O_2 of GCE/PEDOT-PBA-Hematin sensor

The electrocatalytic behavior of GCE/PEDOT-PBA-Hematin towards H_2O_2 was investigated. Catalytic reduction of H_2O_2 at the biosensor was examined by amperometry. The typical current–time plot of GCE/PEDOT-PBA-Hematin is given in **Fig. 6A**. The working potential was set at −0.3 V, which was obtained from Fig. 5. The biosensor responded rapidly when H_2O_2 was successive injected, and it reached a steady state (95% of the maximum value) within 3 seconds, indicating a fast diffusion of the substrate in the hybrid film on the electrode and the high sensitivity of the biosensor. **Fig. 6B** shows the calibration curve of the amperometric response and concentration of H_2O_2. The biosensor has a good linear relationship with H_2O_2 in the range from 0.005 mmol·L^{-1} to 1.322 mmol·L^{-1}: I(μA) =-0.2C(mM)-0.004, with a correlation coefficient of 0.999, the detection limit was estimated to be 0.03 μmol·L^{-1} at a signal-to-noise ratio of 3 and the detection sensitivity is 2.83 μA·mM^{-1}·cm^{-2}, which is much higher than those hydrogen peroxide biosensors based on HRP, Mb and Hb [**Table 1**].

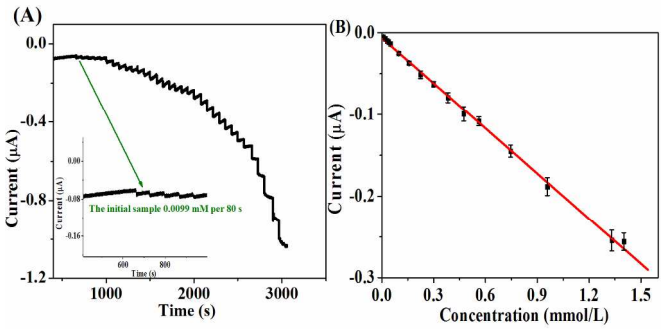

Fig. 6 (A) The current-time curve of GCE/PEDOT-PBA-Hematin to H_2O_2; (B) The linear relationship of current and H_2O_2 concentration; in pH 7.0, 0.1 mol·L^{-1} PBS, with the potential is -0.3 V and the sample time interval is 80s upon initialy successive additions of 0.0099 mmol·L^{-1} H_2O_2 into the stirring PBS and then the addition of H_2O_2 concentration gradually increased. Potentials vs. to Hg/HgCl/Saturated KCl reference electrode.

Modified electrode	Linear range (mM)	Detection limit (μM)(mM)	k_m	Ref.
Mb–GO–Nafion	0.006-0.088	2.5	-	48
ZnO–GNPs–Nafion–HRP	0.015-1.1	9	1.76	49
H-GNs/AuNPs/GCE	0.0003-1.8	0.11	-	50
Nafion/Hb/AuNRs–GOs@Pdop/GCE	0.0036-6	2	0.7	51
Au/GS/HRP/CS/GCE	0.005-5.13	1.7	2.61	52
Nafion/HRP/AgNL/GC	0.039-5.2	0.13	0.32	53
HRP/PTMSPA@GNR	0.01-1	0.06	-	54
MWCNT–CS–He/PAR-GCE	0.001-0.01	0.61	-	39
GCE/PEDOT-PBA-He	0.005-1.322	0.03	0.27	This work

Mb: myoglobin; GO: graphene; Hb: hemoglobin; HRP: horseradish peroxide; H-GNs: hemin-graphene; AuNPs: Au nanoparticles; AuNRs: Au nanorods; GOs@Pdop: graphene oxide sheets (GOs) coated by polydopamine; CS:chitosan; PTMSPA: poly(N-[3-(trimethoxysilyl)propyl]aniline; GNRs: gold nanorods; CMCS: carboxymethyl chitosan; He:hematin; PAR: poly-(acridine red).

Table 1 The performances of various modified electrodes in the detection of H_2O_2

When the concentration of H_2O_2 is higher than 1.322 mmol·L^{-1}, a response plateau in calibration curve is observed, showing the characteristics of the Michaelis–Menten kinetic mechanism.[45] The apparent Michaelis–Menten constant k_m^{app} can be obtained from the electrochemical version of the Lineweaver–Burk equation:$1/I_{ss} = 1/I_{max} + k_m^{app}/I_{max}C$,[46] where I_{ss} is the steady-state current after the addition of substrate, I_{max} is the maximal current measured under saturated substrate conditions, and C is the bulk concentration of the substrate. According to the above equation, the k_m^{app} value for the enzymatic activity of the GCE/PEDOT-PBA-Hematin to H_2O_2 was determined to be 0.269 mmol·L^{-1}. Compared to data obtained for heme proteins immobilized at different devices,[49,52-53] the relatively low value of the K_m^{app} demonstrates the enhancement in the affinity and catalytic activity of hematin grafted to the surface of GCE/PEDOT-PBA. Evidently, the functionalized PEDOT film provides a protective environment for promoting electron transfer. This shows that the immobilized hematin retains its bioelectrocatalytic activity and possesses a high biological affinity toward H_2O_2.

2.7 The reproducibility and stability testing of biomimetic sensors

The long-term stability of our fabricated biosensor was also investigated by examining its current response during storage in a refrigerator at 4℃. The biosensor exhibited no obvious decrease in current response in the first week and maintained about 92% of its initial value after 5 weeks. The repeatability of the measurement was

tested by using the same electrode detecting 0.08 mmol·L^{-1} H_2O_2 for 8 times, its relative standard deviation (RSD) was found to be 3.6%. Five electrodes were treated with same method to check the reproducibility of the biosensor by testing H_2O_2 of 0.08 mmol·L^{-1}, results revealed a RSD of 4.2%, which is acceptable.

2.8 The practical application of biomimetic sensors

To evaluate the ability of the sensor for routine analysis, the sensor was applied to the determination of H_2O_2 in blood serum samples and also a commercial oxidant solution. The actual concentration of H_2O_2 in the oxidant solution was determined by the $KMnO_4$ titration method and also by using the GCE/PEDOT/PBA/Hematin biosensor prepared in the experiment.[47]Results are presented in Table 2, the ratio of the two test facility to H_2O_2 in real samples is between 0.8-1.07, which shows that there is a very good agreement between the results obtained for the commercial oxidant solution by the proposed sensor and those obtained by the $KMnO_4$ titration method. The results also show good reproducibility.

Sample	Added(μM)	Found by $KMnO_4$(μM)	Detected by biosensor(μM)	Ratio of the the two recovery
Blood serum	-	0	0	-
	20	21.5	23.1	1.07
	50	48.2	50.2	1.04
	100	103.4	110.4	1.07
Qxidant	-	0	0	-
	20	23.8	18.9	0.80
	50	51.2	52.0	1.01
	100	97.6	96.9	0.99

Table 2 Results of analysis of H_2O_2 in real sample

3 Conclusions

A novel biosensor was successfully fabricated by modifying GCE with PEDOT, PBA and hematin. This GCE/PEDOT-PBA-Hematin biosensor showed a better electrocatalytic activity to H_2O_2 compared to those enzyme modified electrodes [table 1]. It could be deduced that the increased catalytic response was due to the enlarged specific surface area of the electrode, and the higher electron transfer rate of the PEDOT; hence, an improved synergistic catalytic effect was observed between the hematin and GCE. Satisfactory performance of the biosensor was attributed to its high sensitivity, good stability and reproducibility, wide linear response range, short response time and high analyte specificity. It is very sensitive and could be used to detect trace amounts of H_2O_2 in the range of 0.005-1.322 mmol·L^{-1}.The method proposed in this paper can also be expanded to detect oxygen、peroxide、nitric oxide, and so on.

Acknowledgements

We are grateful to Nanjing University of Science and Technology for its start-up funding, National Natural Science funding (No. 21345002) for this project.

Notes and references

[1]School of Environmental and Biological Engineering
Nanjing University of Science & Technology
No. 200 Xiaolingwei, Xuanwu District, Nanjing, P. R. China 210094
[2]State Key Laboratory of Urban Water Resource and Environment,
School of Chemical Engineering and Technology,
Harbin Institute of Technology, Harbin 150001, China.
[3]Chemistry Department, College of Arts and Sciences
University of South Florida, 4202 East Fowler Ave, Tampa, FL, 33620
Corresponding Author: Jinming Kong, Xueji Zhang
Email: j.kong@njust.edu.cn,xueji@usf.edu†

1 L. Kesavalu, S. C. Holt and J. L. Ebersole, Oral Microbiol.Immunol. 2003, 18, 226.
2 M. T. de Groot, M. Merkx, Ad H. Wonders and T. M Marc, J. Am. Chem. Soc. 2005, 127, 7579.
3 Z. X. Liang, H. Y. Song and S. J. Liao, J. Phys. Chem. C, 2011, 115, 2604.
4 W. Wen, W. Chen, Q. Q. Ren, X. Y. Hu, H. Y. Xiong, X. H. Zhang, S. Fu and Y. D. Zhao Wang, Sens Actuators B, 2012, 166–167, 444.
5 Y. F. Gao and J. Y. Chen, J. Electroanal. Chem., 2005, 583, 286.
6 Q. Q. Guo, S. J. Ji, Q. L. Yue, L. Wang, J. F. Liu, Anal. Chem.,2009, 81, 5381.
7 T. Xue, S. Jiang, Y. Q. Qu, Q. Su, R. Cheng, S. Dubin, C. Y. Chiu, R. Kaner, Y. Huang and X. F Duan, Angew. Chem. 2012, 124, 3888.
8 J. Chen, L. Zhao, H. Bai and G. Q. Shi, J Electroanal Chemy, 2011, 657, 34.
9 Y. J. Guo, J. Li and S. J. Dong, Sens Actuators B, 2011, 160, 295.
10 R. Z. Jiang, D. T.Tran, J. McClure and D. Chu, Electrochem Commun, 2012, 19, 73.
11 Q. Ma, S. Y. Ai, H. S. Yin, Q. P. Chen and T. T. Tang, Electrochimica Acta. 2010, 55, 6687.
12 R. J. Chen, Y. G. Zhang, D. W. Wang and H. J. Dai, J. Am. Chem. Soc. 2001,123, 3838-3839.
13 H. Jaegfeldt, T. Kuwana and G. Johansson, J. Am. Chem. Soc. 1983, 105, 1805.
14 K. S. Subrahmanyam, A. Ghosh, A. Gomathi, A. Govindaraj and C. N. R. Rao, Nanosci Nanotechnol Lett. 2009, 1, 28.
15 F. E. Bernard, B. X. Chen; M. Zhu and Louis, B. Nano lett. 2001, 1, 465.
16 S. R. Guo, J. Lin, M. Penchev, E. Yengel, M. Ghazinejad, C. Ozkan and M. Ozkan, J Nanosci Nanotechno. 2011, 11, 5258.
17 B. Koen, L. Jeong-O, G. M. Frank, H. H. Wiertz and D. Cees, Nano lett. 2003, 3, 727.
18 F. Jonas and L. Schrader, Synth. Met. 1991, 41–43, 831.
19 D. J. Heywang and D. F. Jonas, Adv. Mater. 1992, 4, 116.
20 J. Roncali, P. Blanchard, P. Frère. J. Mater. Chem., 2005, 15, 1589.
21 R. W. Gerald, J. W. Timothy, F. Michael, Transition Met.Chem., 23, 1998, 467.
22 N. Guillaume, O. B. Isa, G. Isabelle, P. Muriel, L. Jean, D. Didier, T. Charles, R. T. Daniel and B. Bruno, J. Am. Chem. Soc. 2004, 126, 1497.
23 J. M. Kong, A. R. Ferhan, X. T. Chen, L. Zhang and N. Balasubramanian, Anal. Chem. 2008, 80, 7213.
24 C. T. Buscher, D. M. Branch and D. Q. Li, J. Am. Chem. Soc. 1996, 118, 2950.

25 P. Wentworth Jr, L. H. Jones, A. D. Wentworth, X. Zhu, N. A. Larsen, I. A. Wilson, X. Xu, W. A. Goddard, K. D. Janda, A. Eschenmoser and R. A. Lerner, Science, 2001, 293, 1806.
26 V. Thome-Duret, G. Reach, M. N. Gangnerau, F. Lemonnier, J. C.mKlein, Y. Zhang, Y. Hu, G. S. Wilson, Anal. Chem. 1996, 68, 3822.
27 W. Chen, S. Cai, Q. Q. Ren, W. Wen and Y. D. Zhao, Analyst. 2012, 137, 49.
28 Zhao, W. J.; Wang, Zh. H.; Li, Q. M.; Anal. Methods, 2012, 4, 1105.
29 W. M. Si, W. Lei, Y. H. Zhang, M. Z. Xia, F. Y. Wang and Q. L. Hao, Electrochimica Acta. 2012, 85, 295 (the reference of supporting information).
30 H. Y. Song, Y. N. Ni and S. Kokot, Analytica Chimica Acta. 2013, 788, 24.
31 J. E. B. Discuss. Faraday Soc. 1947, 1, 11.
32 F. Patolsky, M. Zayats and E. Katz and I. Villner, Anal. Chem. 1999, 71, 3171.
33 A. J. Bard and L. R. Faulkner, Electrochemical Methods: Fundamentals and Applications, second ed., John Wiley, New York, 2000.
34 L. Yang and Y. Li, Biosens. Bioelectron. 2005, 20, 1407.
35 H. Huang, Z. Liu and X. Yang, Anal. Biochem. 356 (2006) 208.
36 Q. Ma, S. Y. Ai, H. S. Yin, Q. P. Chen and T. T. Tang, Electrochim. Acta. 2010, 55, 6687.
37 H. Aoshima, Y. Yoshida and H. Taniguichi, Agric. Biol. Chem. 1986, 50, 1777.
38 B. J. Reeder and M. T. Wilson. Free Radical Bio Med, 2001, 30, 1311.
39 G. Ran, W. J. Yi, Y. Li, H. Q. Luo and N. B. Li, Anal. Methods, 2012, 4, 2929.
40 E. Laviron, J. Electroanal. Chem., 1979, 100, 263.
41 S. F. Wang, T. Chen, Z. L. Zhang, X. C. Shen, Z. X. Lu, D. W. Pang and K. Y. Wong, Langmuir. 2005,21, 9260.
42 D. L. Compton and J. A. Laszlo J. Electroanal. Chem. 2002, 520, 71.
43 S. H. Ma, X. J. Wang and X. J. Han, Chinese Journal of Analytical Chemistry. 2013, 41.
44 A. F. E. Nassar, Z. Zhang, N. Hu, J. F. Rusling and T. F. Kumosinski. J. Phys. Chem. B, 1997,101, 2224.
45 R. A. Kamin and G. S. Wilson, Anal.Chem. 1980, 52, 1198.
46 X. Shangguan and J. Zheng, Electroanal. 2009, 21, 881.
47 A. I. Vogel, Vogel's Textbook of Quantitative Chemical Analysis, fivth ed.,Longman, New York, 1989, 372
48 C. C. Guo, H. Sun and X. S. Zhao, Sens. Actuators, B, 2012, 164,82.
49 C. L. Xiang, Y.J. Zou, L.X. Sun and F. Xu, Sens. Actuators B, 2009, 136, 158.
50 H. Y. Song, Y. N. Ni, S. Kokot. Analytica Chimica Acta. 2013, 788, 24.
51 C. Wang, X. C. Zou, Q. Wang, K. Shi, J. Tan, X. Zhao, Y. Q Chai and R. Yuan. Anal. Methods, 2014, 6, 758.
52 K. F. Zhou, Y. H. Zhu, X. L. Yang, J. Luo, C. Z. Li and S. R. Luan, Electrochimica Acta. 2010, 55, 3055.
53 A. S. Rad, M. Jahanshahi, M. Ardjmand and A. A. Safekordi, Int. J. Electrochem. Sci. 2012, 7, 2623.
54 S. Komathi, A. L. Gopalan, S. K. Kima, G. S. Anand and K. P. Lee. Electrochimica Acta. 2013, 92, 71.